Topics in Heavy Ion Collisions, Montreal, Canada, June 25-28, 2003

Saturation at RHIC

Elena G. Ferreiro
with C. Pajares

Departamento de Física de Partículas
Universidade de Santiago de Compostela,
Spain

Contents:

1. Introduction: Parton saturation. Models for the initial state

2. The Colour Glass Condensate (with E. Iancu, L. McLerran, K. Itakura, A. Leonidov)

3. Phase transition?: Percolation of strings (with N. Armesto, M.A.Braun, F.del Moral and C. Pajares)

1. INTRODUCTION:
Parton saturation at small x

• Recent years: Growing activity around systems and experiments DIS at HERA, heavy-ion experiments at RHIC involving large number of partons due to high energy and high number of participants

• Main problem: High parton densities. At high energy the QCD cross sections are controlled by small x gluons in the hadron wavefunction, whose density grows rapidly with the energy (or with decreasing Bjorken's x) due to the enhancement of radiative process.

• Perturbation QCD: By resumming dominant radiative corrections at high energy, the BFKL eq. leads to a gluon density that grows like a power of s $\Rightarrow$ σ also grows like a power of s and violates Froissart bound.

• BFKL and DGLAP: Linear equations that neglet the interaction among the small x gluons

With increasing energy, recombination effects favoured by the high density of partons should become more important and lead to eventual saturation of the parton densities.

• Some models for the initial state:

1. pQCD based: HIJING, VNI (cascade), AMPT, (final state) saturation (Eskola et al.).
2. String models: Fritiof, DPM/QGSM (DPMJET, SFM→PSM, NEXUS), RQMD, UrQMD, HSD.
3. Statistical models: QGP.
4. High-density QCD. CGC: Kharzeev et al., Pirner et al., Krasnitz et al. (lattice).

$$\frac{dN^{ch}_{AA}}{d\eta}(b) = a(\eta, b)N_{part}(b) + c(\eta, b)N_{coll}(b).$$

A) $N_{part}(b) \propto A$: number of participant nucleons, valence-like contribution.
B) $N_{coll}(b) \propto A^{4/3}$: number of inelastic nucleon-nucleon collisions (not only hard), dominant at asymptotic energies (AGK cancellation).

• A) is the only contribution in WNM. Some models provide a recipe for the contribution of B): HIJING, DPM/QGSM.

• To get the right multiplicities at RHIC, some mechanisms to lower the contribution of B) (but not enough to get WNM) have been introduced:

1. Very strong shadowing of gluon distributions in nuclei in HIJING (S.-Y.Li et al., PLB527 (02) 85).

2. Geometrical parton saturation (K.J.Eskola et al, NPB570 (00) 379):

$$N(p_0)\frac{\pi}{p_0^2} \leq \pi R_A^2. \qquad (1)$$

3. Pomeron interaction in DPM (A.Capella et al., PLB511 (01) 185).

4. **Saturation in high-density QCD: CGC** (D.E.Kharzeev et al., PLB507 (01) 121; B523 (01) 79).

5. **Interaction/percolation of strings**.

All these mechanisms have in common the presence and/or modification of a multiple scattering pattern (in the target rest frame) or gluon interaction (in a fast moving frame).

THE COLOUR GLASS CONDENSATE

(Iancu, Leonidov, McLerran, Itakura, Ferreiro)

• Non-linear effects in the hadron wavefunction become important when the interaction probability for the gluons becomes of $\mathcal{O}(1)$ (gluons overlap):

$$\frac{\alpha_s N_c}{Q^2} \times \frac{xG(x,Q^2)}{\pi R^2} \sim 1$$

Transverse size of the gluon Density of gluons

• Equiv: For a given energy, saturation occurs for those gluons having a sufficiently large transverse size $r_\perp^2 \sim 1/Q^2$, larger than a critical value $1/Q_s(x) \Rightarrow$

$\Rightarrow$ Gluons with momenta $Q^2 \lesssim Q_s^2(x)$ where

$$Q_s^2(x) = \alpha_s N_c \frac{xG(x,Q_s^2)}{\pi R^2} \equiv \frac{(\text{colour charge})^2}{\text{area}}$$
$$\sim A^{1/3} x^{-\lambda\alpha_s}$$

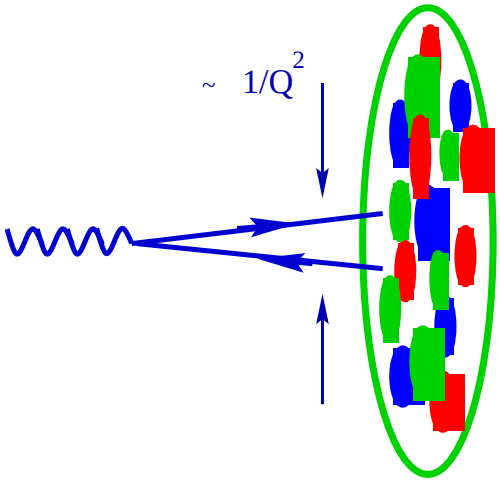
~ 1/Q2

• For sufficiently large energy (x small enough):

$$\boxed{Q_s^2(x) \gg \Lambda_{QCD}^2 \,\text{and}\, \alpha_s(Q_s) \ll 1}$$

$\Rightarrow$ Weak coupling QCD

• But although the coupling is small the effects of the interactions are amplified by the large gluon density:
At saturation: $xG(x, Q_s^2) \sim 1/\alpha_s \gg 1 \Longrightarrow$
large ocupation numbers
semi-classical regime [McLerran, Venugopalan (94)]
ordinary perturbation theory breaks down

• Our strategy: To construct an effective theory in which the small-x gluons are describe by classical colour fields radiated by a random colour source, that of the fast partons with larger x

• The advantage: Non-linear effects in a classical context $\Rightarrow$ Exact calculations are possible
For the fast partons and their mutual interactions: Perturbation theory for the quantum corrections

Phenomenology at RHIC

(Kharzeev, Levin, Nardi, 2001; McLerran, Schaffner-Bielich, Venugopalan, 2001)

CGC: Appropiate description of the initial conditions at RHIC

Density of partons at saturation:

$$xG(x,Q_s^2) = \frac{\pi R_A^2\, Q_s^2(x,A)}{\alpha_s(Q_s^2)} \sim \ln N_{part}$$

- $\pi R_A^2 \propto N_{part}^{2/3}$ = the nuclear overlap area
- $Q_s^2(x,A) \propto N_{part}^{1/3}$ = the saturation momentum
- $1/\alpha_s(Q_s^2) \approx \ln(Q_s^2/\Lambda_{QCD}^2) \sim \ln N_{part}$

Transverse momentum spectra at saturation:

Intrinsic p_T broadening in the partonic phase

$$< p_T >^2 \sim \frac{1}{\pi R_A^2}\frac{dN}{dy}$$

Scaling relations:

$$\frac{1}{\sigma}\frac{dN}{d\eta d^2p_T} = \frac{1}{\alpha_s} f(\frac{p_T^2}{Q_s^2}) \qquad \frac{1}{\sigma}\frac{dN}{dy d^2m_T} = \frac{1}{\alpha_s} f(\frac{m_T}{Q_s^2})$$

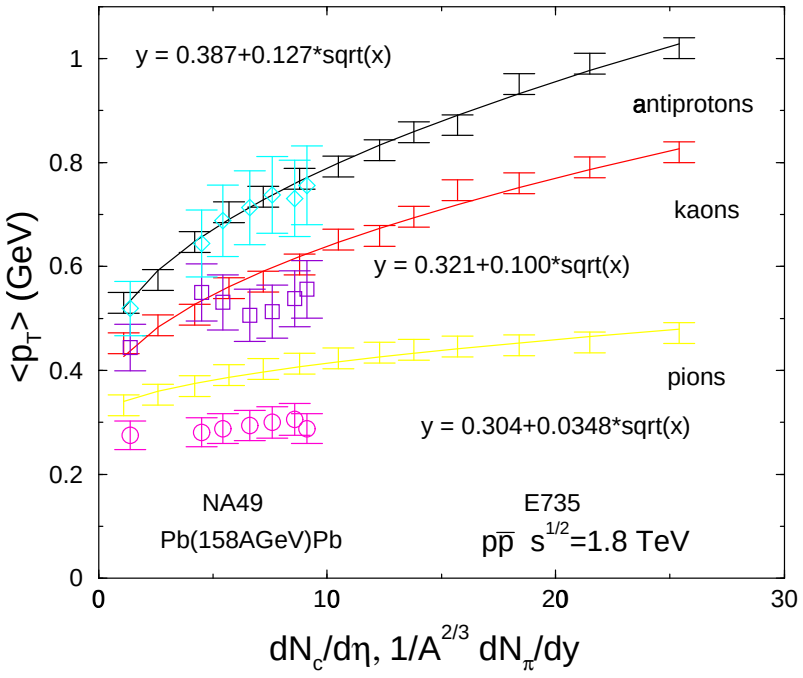

Solid curves: Two parameters fits $< p_T >=< p_T >_0 + \frac{1}{\sigma}\sqrt{\frac{dN}{dy}}$

Coefficients of $\sqrt{\frac{dN}{dy}}$ and the value of $< p_T >$ as $\frac{dN}{dy}$ goes to zero

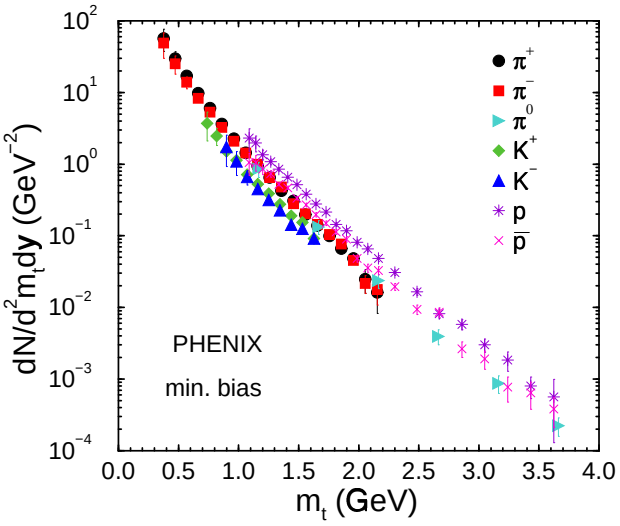

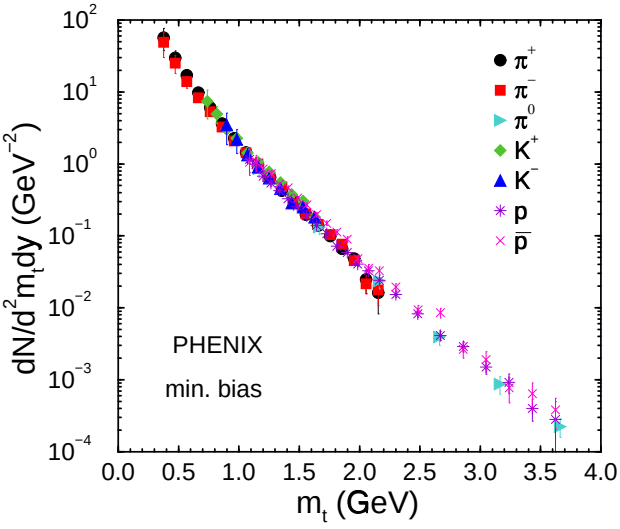

Data points for all hadrons seem to follow one curve. k and p diverge due to the quantum numbers that are not taken into account in the scaling relation

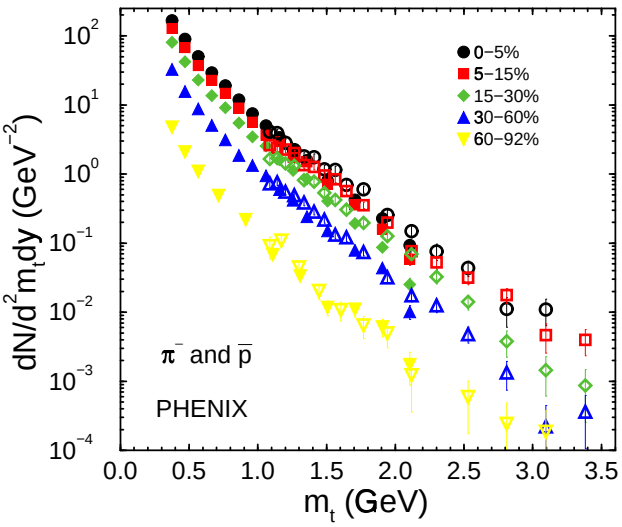

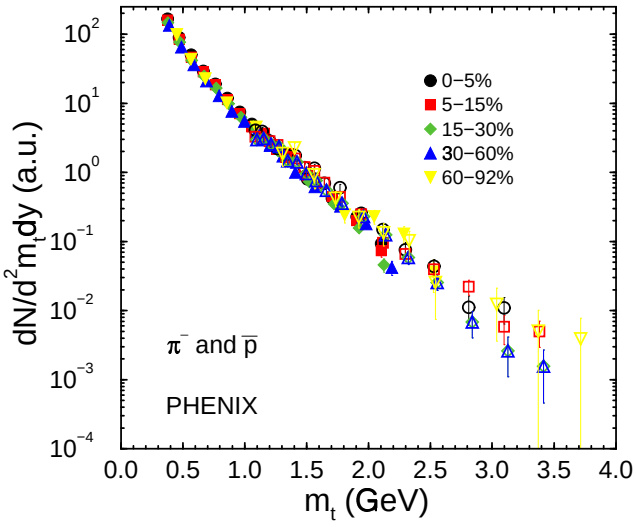

Universal curves for each centrality bin, even for the most peripheral one. Moreover, there is only one scaling function and the m_T spectra for different centralities can be rescaled into each other by properly choosing σ and Q_s for each centrality bin

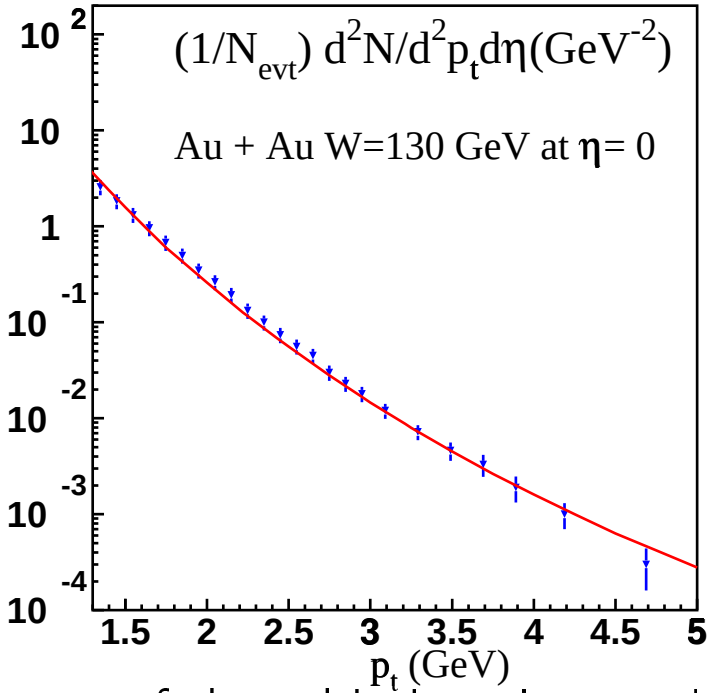

The p_T spectrum of charged hadrons in central Au-Au collsions at $\sqrt{s} = 130$ GeV.

At saturation:

$$\frac{dN}{dyd^2p_T} \sim \frac{\pi R_A^2 Q_s^2}{p_T^2} \longrightarrow \frac{N_{part}}{p_T^2}$$

$$\frac{dN}{dyd^2p_T} \sim \frac{1}{p_T^2} xG(x,Q^2) \sim$$

Large p_T: $\frac{1}{p_T^2}$ (Bremsstrahlung)

Small p_T: $\ln \frac{Q_s^2}{p_T^2}$

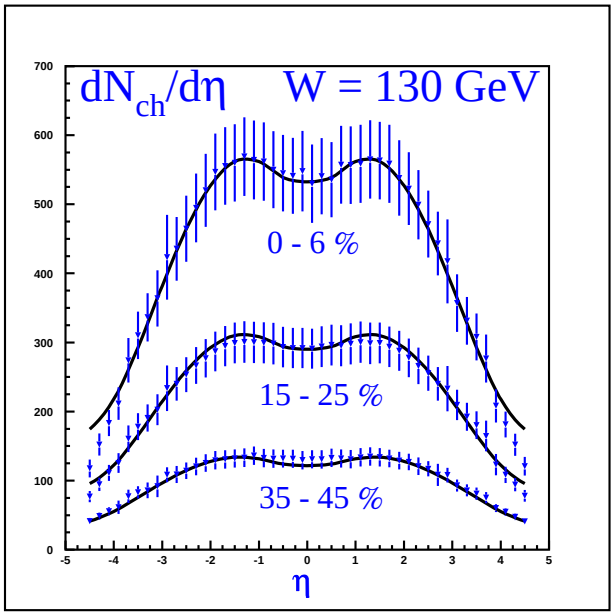
dN$_{ch}$/dη W = 130 GeV
0 - 6 %
15 - 25 %
35 - 45 %
η

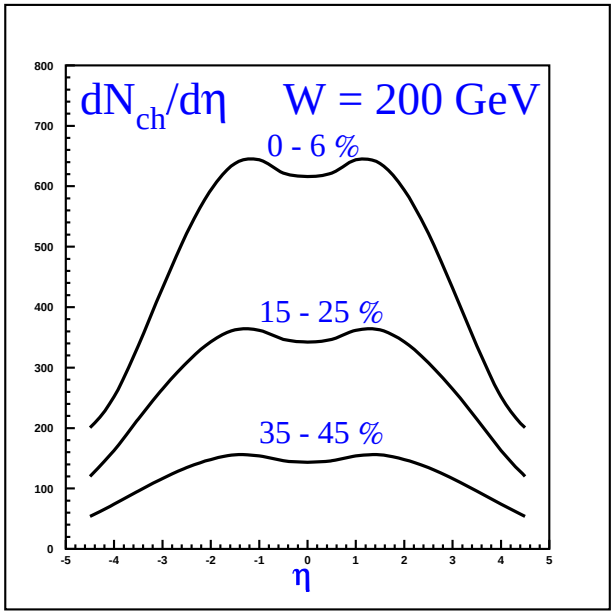
dN$_{ch}$/dη W = 200 GeV
0 - 6 %
15 - 25 %
35 - 45 %
η

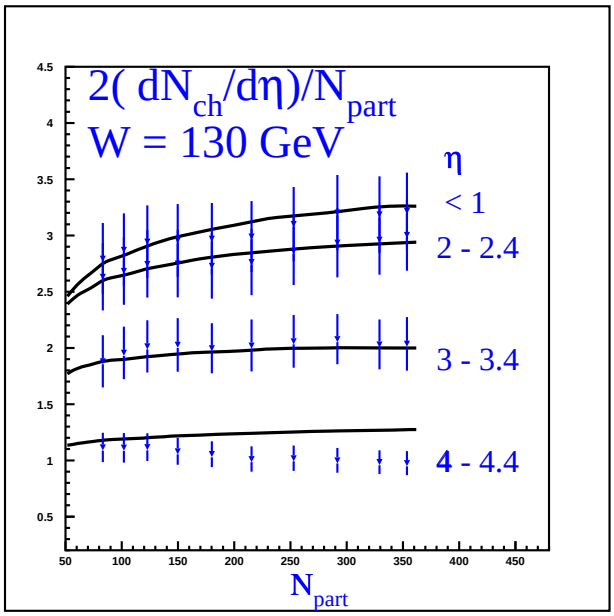
2(dN$_{ch}$/dη)/N$_{part}$
W = 130 GeV
η
< 1
2 - 2.4
3 - 3.4
4 - 4.4
N$_{part}$

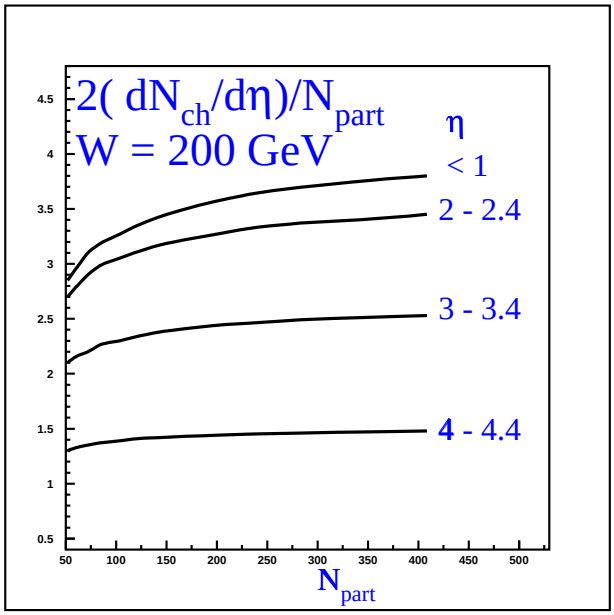
2(dN$_{ch}$/dη)/N$_{part}$
W = 200 GeV
η
< 1
2 - 2.4
3 - 3.4
4 - 4.4
N$_{part}$

STRING MODELS: PERCOLATION

(Armesto, Braun, Moral, Pajares, Ferreiro)

• Color strings are stretched between the projectile and target

• Hadronization of these strings produces the observed hadrons

• Color strings = Small areas in the transverse space filled with color field created by the colliding partons

• Particles are created via emission of $q\bar{q}$ pair in this field

• With growing energy and/or atomic number of colliding particles, the number of strings grows

• So the strings start to overlap, forming clusters, very much like disk in the 2-dimensional percolation theory

• In particular, at a certain critical density, a macroscopic cluster appears, which marks the percolation phase transition

• So we try to introduce a phase transition (≡QGP?) (NSA et al., PRL77 (96) 3736; M.A.Braun et al., PRC65 (02) 024907; J.Dias de Deus et al., PLB491 (00) 253; 494 (00) 53).

• How?: Strings fuse forming clusters. At a certain critical density η_c (central PbPb at SPS, central AgAg at RHIC, central SS at LHC) a macroscopic cluster appears which marks the percolation phase transition (second order, non thermal).

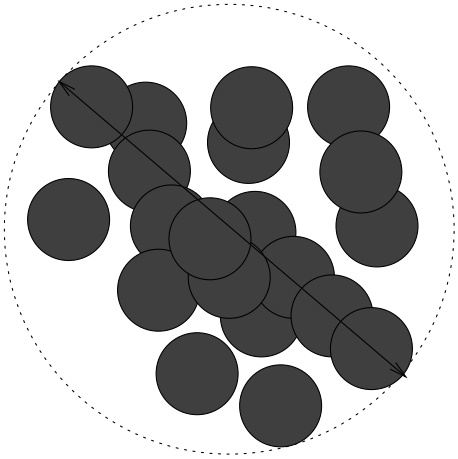

$$\eta = N_{st}\frac{S_1}{S_A}\ , \quad S_1 = \pi r_0^2, \quad r_0 = 0.2 \ \text{fm}, \quad \eta_c = 1.1 \div 1.5.$$

• Hypothesis: clusters of overlapping strings are the sources of particle production, and central multiplicities and transverse momentum distributions are little affected by rescattering.

• For a cluster of n overlapping strings covering an area S_n:

Color charge of the cluster=Vectorial sum of the strings charges

$$\vec{Q}_n = \sum_{i=1}^{n} \vec{Q}_{1i}, \quad \langle \vec{Q}_{1i} \cdot \vec{Q}_{1j} \rangle = 0, \quad \vec{Q}_n^2 = n\vec{Q}_1^2, \qquad (2)$$

$$Q_n = \sqrt{\frac{nS_n}{S_1}} Q_1, \quad \mu_n = \sqrt{\frac{nS_n}{S_1}} \mu_1, \quad \langle p_T^2 \rangle_n = \sqrt{\frac{nS_1}{S_n}} \langle p_T^2 \rangle_1. \qquad (3)$$

For strings without interaction: $S_n = nS_1$, $Q_n = nQ_1 \rightarrow$ $\mu_n = n\mu_1$, $\langle p_T^2 \rangle_n = \langle p_T^2 \rangle_1$

For strings with max overlapping: $S_n = S_1$, $Q_n = \sqrt{n}Q_1 \rightarrow$ $\mu_n = \sqrt{n}\mu_1$, $\langle p_T^2 \rangle_n = \sqrt{n}\langle p_T^2 \rangle_1$

• With this interpolation, one gets for a cluster the following scaling law with the multiplicity (black area in CGC):

$$\langle p_T^2 \rangle_{AA} = \frac{S_1}{S_{AA}} \frac{\langle p_T^2 \rangle_1}{\mu_1} \mu_{AA}. \qquad (4)$$

Saturation limit: All strings overlap into a single cluster that occupies the whole interaction area

• Moreover, in the limit of high density η, one obtains analytic expression:

$$< \frac{nS_1}{S_n} >= \frac{\eta}{1-\exp(-\eta)} \equiv \frac{1}{F(\eta)^2} \qquad (5)$$

so

$$\mu = N_{strings} F(\eta) \mu_1 \ , \qquad < p_T^2 >= \frac{1}{F(\eta)} < p_T^2 >_1 \quad (6)$$

• We are going to use these relations to compute the multiplicity and transverse momentum distributions

• The multiplicity distribution can be expressed as a superposition of Poisson distributions with different mean multiplicities:

$$P(n) = \int dN \; W(N) \; P(N, n) \tag{7}$$

where the Poisson distribution $P(N, n) = \frac{\mathrm{e}^{-N} N^n}{n!}$, $N =< n >$, represents the cluster fragmentation, while the weight factor $W(N)$ reflects the cluster size distribution

• For the transverse momentum distribution

$$f(m_t) = \int W(x) \; f(x, m_T) \tag{8}$$

where again the weight function $W(x)$ reflects the cluster size distribution and for $f(x, m_T)$ we assume the Schwinger formula, $f(x, m_T) = \exp(-m_T^2 x)$, used also for the fragmentation of a Lund string, where x is related to the string tension, or equivalently to mean transverse size of the string.

• The weight function $W(x)$ reflects the cluster size distribution, and it is well approximated by a gamma distribution

$$W(x) = \frac{\gamma}{\Gamma(k)} (\gamma x)^{k-1} \; \exp\left(-\gamma x\right) \; . \tag{9}$$

• A very similar shape has been obtained in the next-to-next-leading-log approximation in QCD Yu. L. Dokshitzer, Phys. Lett. **B305**, 295 (1993):

$$W(x) = \frac{\mu D}{\Gamma(k)}(Dx)^{k\mu-1}\exp{(-Dx)^{\mu}} \qquad (10)$$

• Introducing the cluster size distribution we obtain for the multiplicity distribution

$$\frac{\Gamma(n+k)}{\Gamma(n+1)\Gamma(k)}\frac{\gamma'^{k}}{(1+\gamma')^{n+k}} \qquad (11)$$

and for the transverse mass distribution

$$\frac{1}{(1+\frac{m_T^2}{\gamma})^{k}} \qquad (12)$$

• The distribution obtained in (11) is the well known negative binomial distribution, whose mean value and dispersion verify:
$< n >=< N >=\frac{k}{\gamma'}$, $\frac{<N^2>-<N>^2}{<N>^2} = \frac{1}{k}$, $\frac{<n^2>-<n>^2}{<n>^2} = \frac{1}{k} + \frac{1}{<n>}$

• In (12) the corresponding values are:
$< x >= \frac{k}{\gamma}$, $\frac{<x^2>-<x>^2}{<x>^2} = \frac{1}{k}$.

• The weight function is invariant under transformations $x \to \lambda x$ and $\gamma \to \gamma/\lambda$. Nevertheless that leads to a change in the distributions. Taking into account the effect of percolation, $\lambda = F(\eta)$

• The multiplicity distribution becomes the universal function

$$\frac{\Gamma(n+k)}{\Gamma(n+1)\Gamma(k)} \frac{(\gamma'/F(\eta))^k}{(1+(\gamma'/F(\eta)))^{n+k}} \tag{13}$$

and the transverse mass distribution behaves as

$$\frac{A}{(\gamma + F(\eta)\ m_T^2)^k} \tag{14}$$

• According to this, $k \sim 1/F(\eta)$ and taking into account the dependence on $\mu = 1/(1-\sqrt{\alpha_s})$, $k \sim \mu$ (Eq. 10)

$$k = \mu(\frac{3}{2} + \frac{1}{F(\eta)}) \tag{15}$$

• In the new distributions $< p_T^2 >=< p_T^2 >_{old} /F(\eta)$ and $< n >=< n >_{old} F(\eta)$

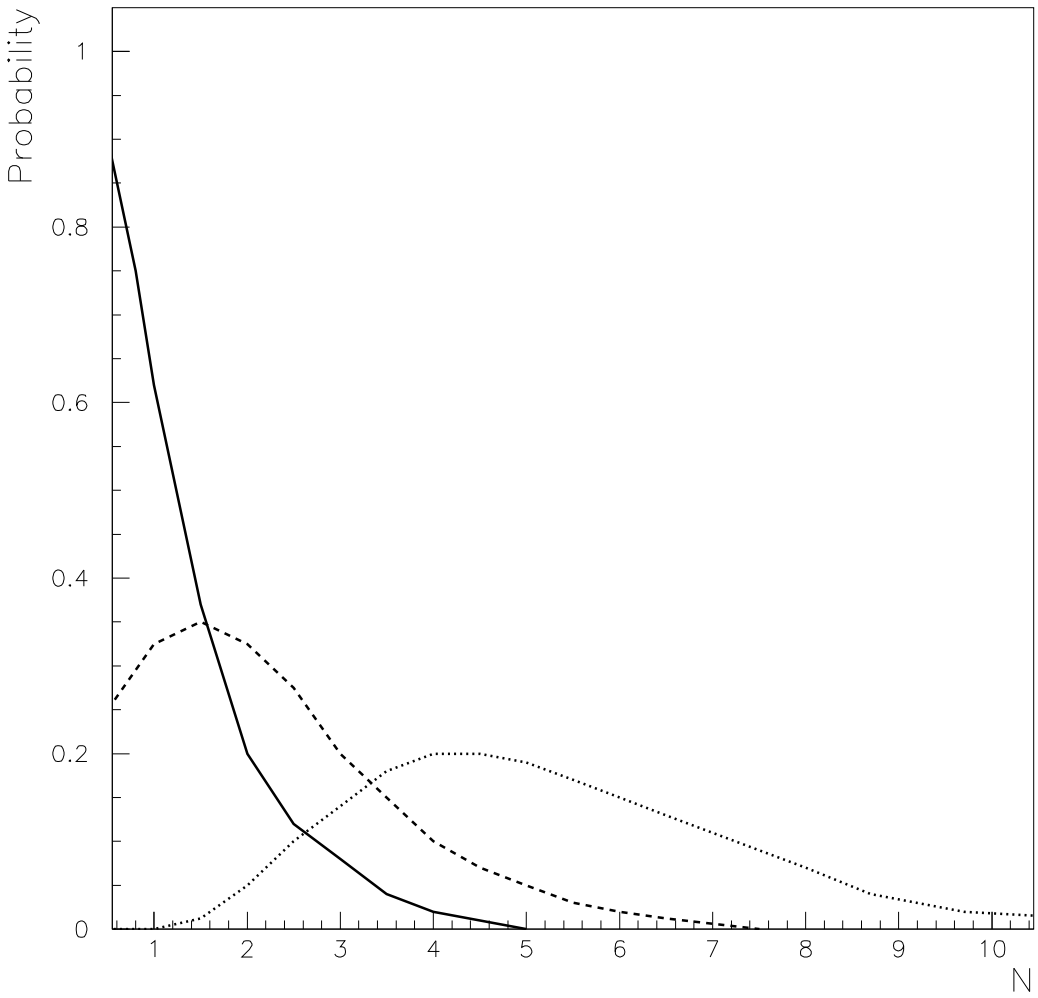

Figure 1: Schematic representation of the number of clusters as a function of the number of strings of each cluster at three different centralities (the continuous line corresponds to the most peripherical one and the pointed line to the most central one)

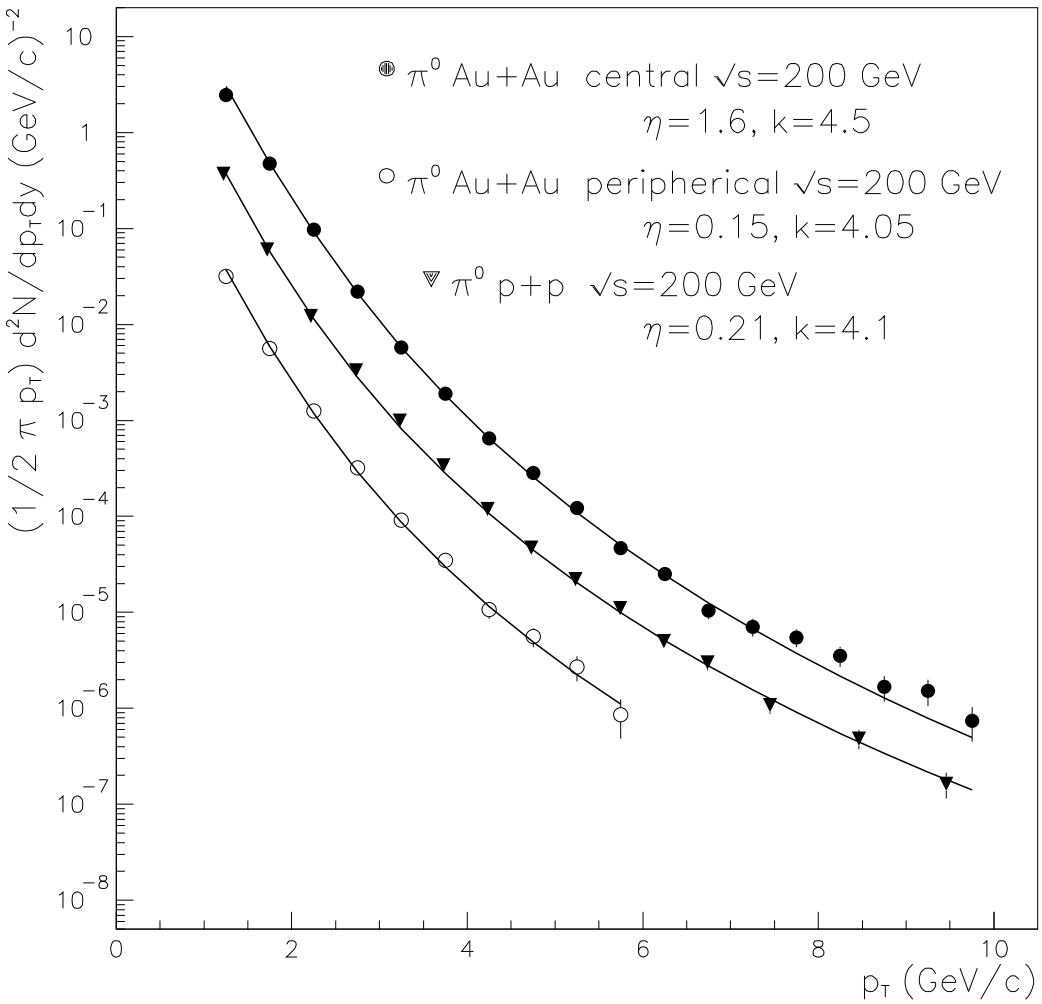

Figure 2: Comparison between our results and experimental data from Au-Au central and peripherical collisions at $\sqrt{s} = 200$ GeV. Data are from PHENIX.

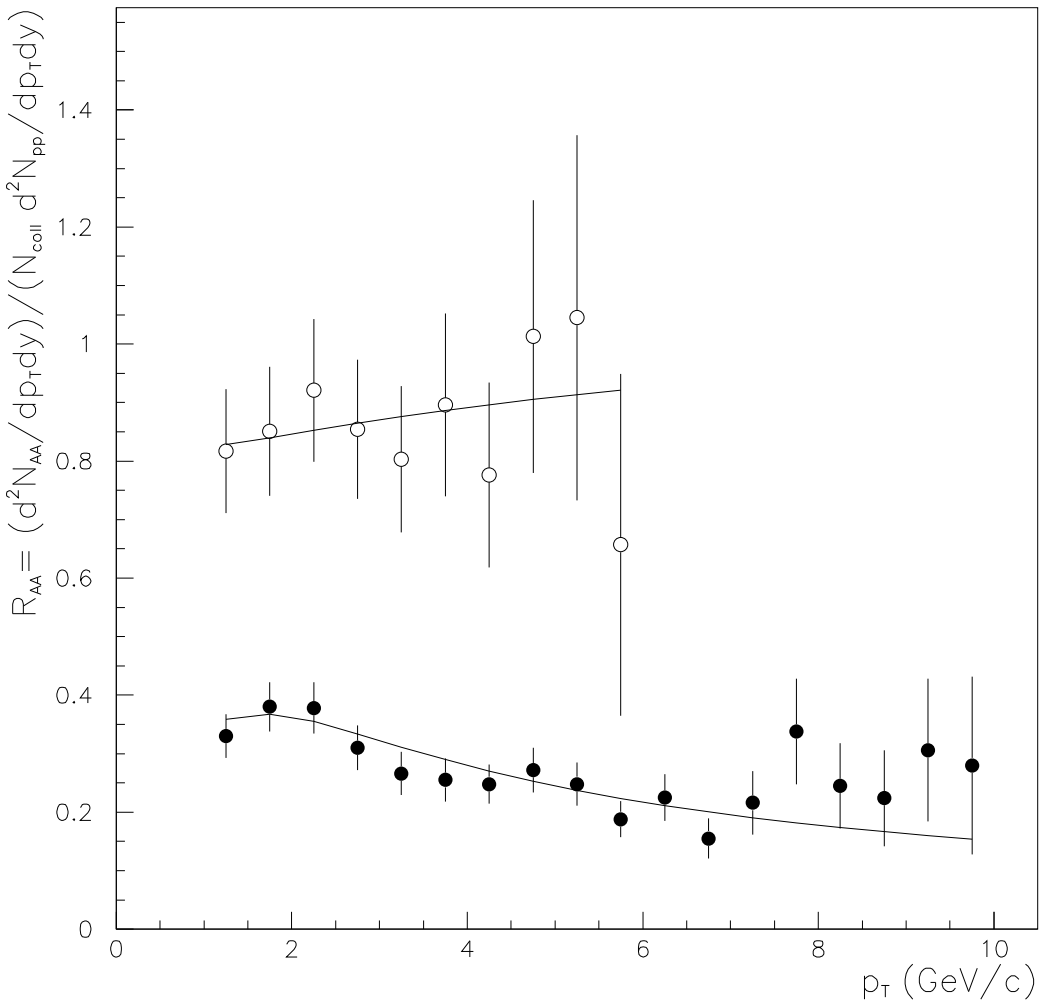

Figure 3: Comparison between our results and experimental data from the nuclear modification factor $R_{AA}(p_T)$ for π^0 in central (closed circles) and peripheral (open circles) Au-Au collisions at $\sqrt{s} = 200$ GeV. Data are from PHENIX.

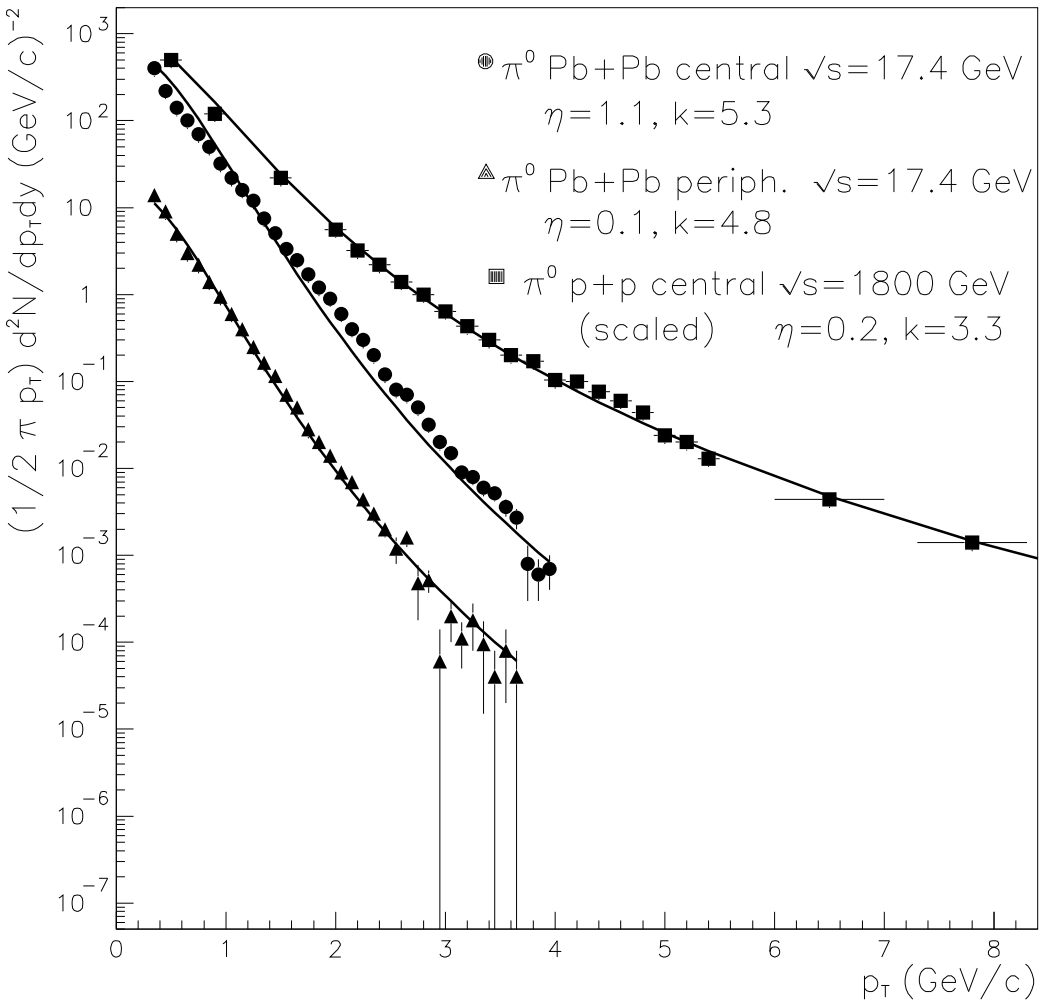

Figure 4: Comparison between our results and experimental data from Pb-Pb central and peripherical collisions at $\sqrt{s} = 17.4$ GeV and p-p collisions at $\sqrt{s} = 1.8$ TeV. Data are from WA98 and CDF.

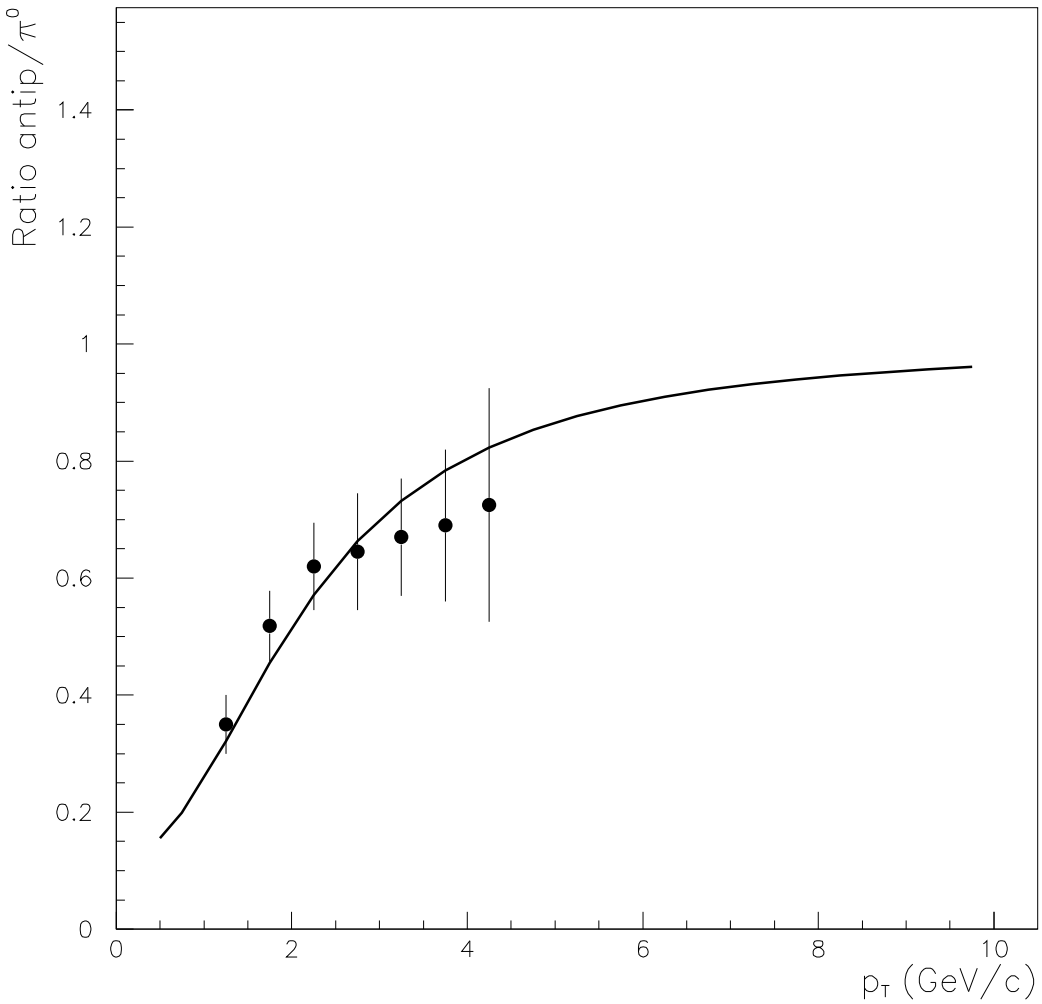

Figure 5: Comparison between our results and experimental data for antiproton/pion^0 for central Au-Au collisions at 200 GeV. Data are from PHENIX.

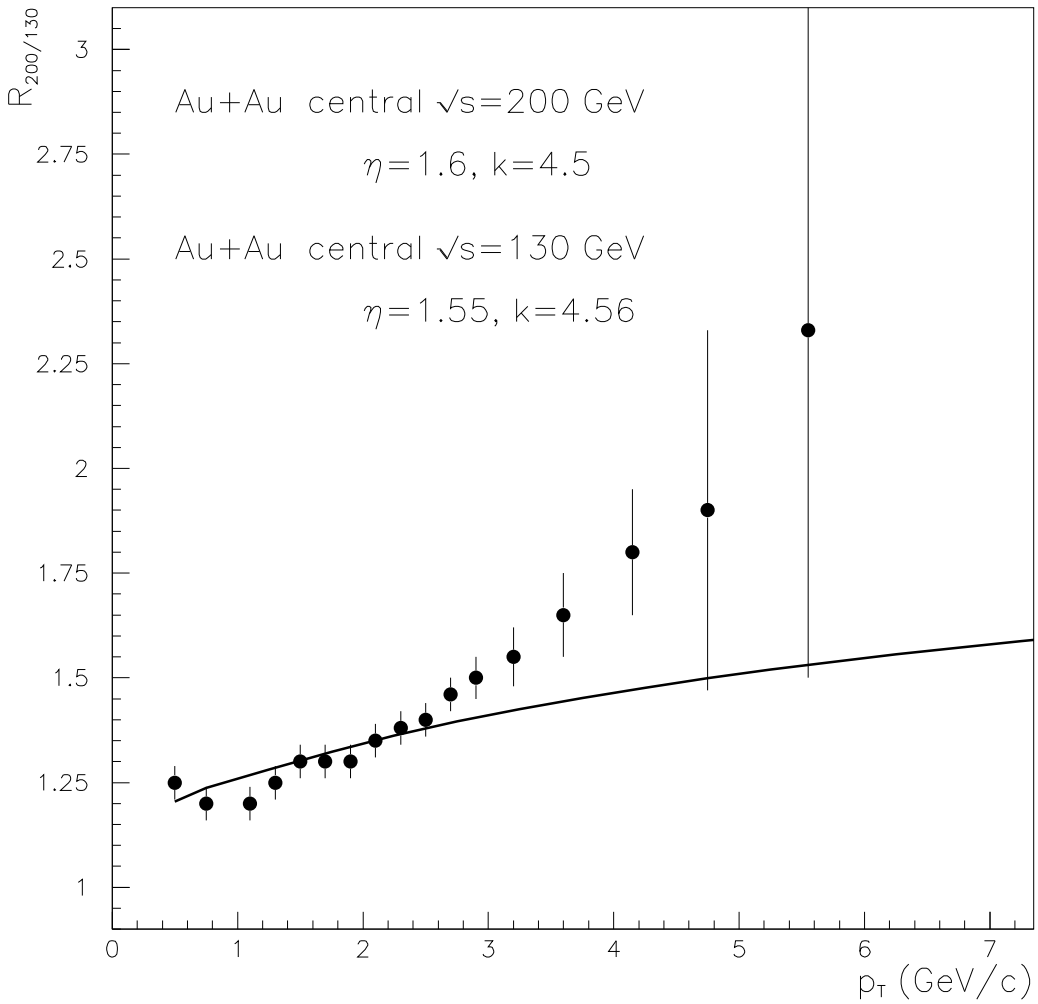

Figure 6: Comparison between our results and experimental data for $R_{200/130}$ for central Au-Au collisions at 200 and 130 GeV. Data are from PHENIX.

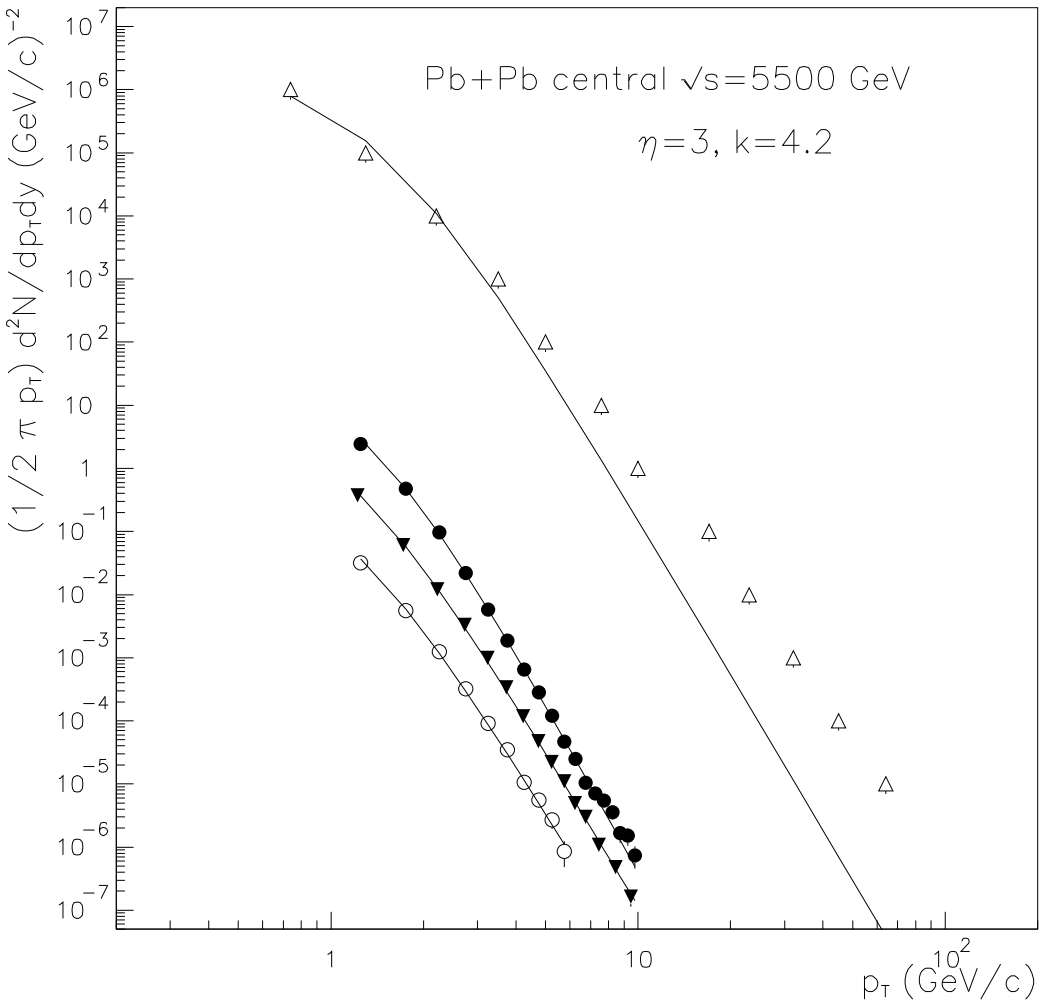

Figure 7: Our results at RHIC for p+p and Au+Au collisions compared with our prediction for Pb+Pb central collisions at LHC energies.

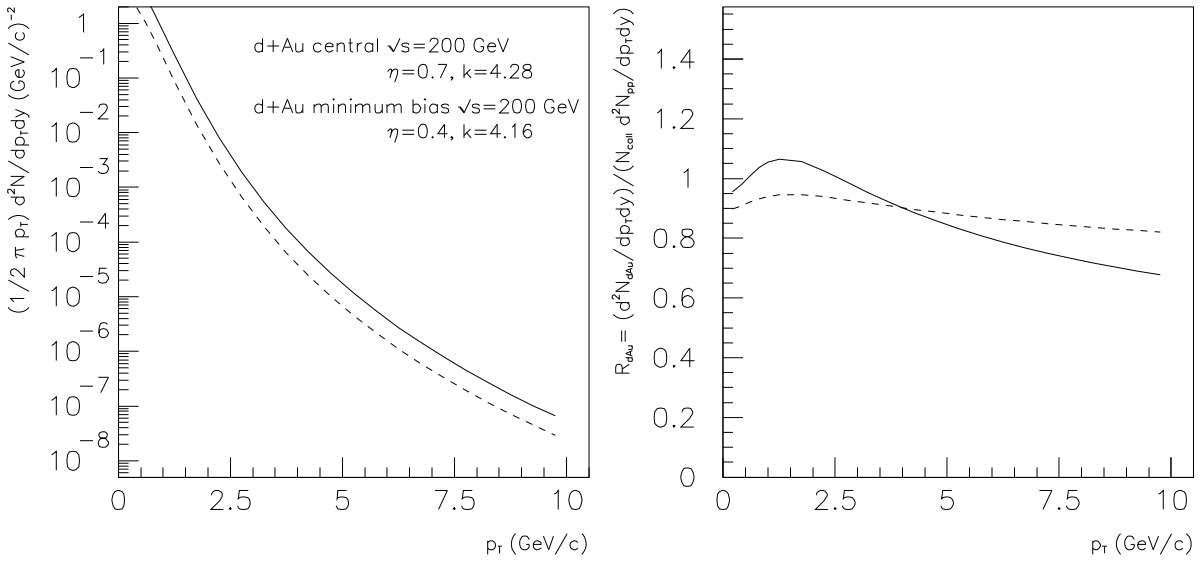

Figure 8: Our prediction for d+Au collisions at 200 GeV and different centralities